

# Modeling Obscurants in an Urban Environment

Donald W. Hooock Jr.  
(505) 678-5430; Fax 678-3385  
dhooock@arl.army.mil

U.S. Army Research Laboratory  
Computational and Information Sciences Directorate  
Battlefield Environment Division  
AMSRD-ARL-CI-ED  
White Sands Missile Range, NM 88002-5501

## ABSTRACT

Line of Sight obscuration effects of smoke, dust and debris on target acquisition are difficult to model in an urban environment. Wind flow and buoyancy in urban street canyons can be complex. This paper outlines the obscuration model being developed by the U. S. Army Research Laboratory for the NATICK RDEC to support the next generation of the Infantry Warrior Simulation (IWARS). It uses the legacy COMBIC obscuration model sources and STATBIC concentration redistribution approach to simulating turbulence effects. The ARL-developed mass-consistent urban 3D Wind Field (3DWF) model is used to provide urban wind field inputs. Various techniques are described to adjust aerosol cloud concentrations for the effects of buildings as they confine the cloud to the streets.

## 1. INTRODUCTION

Models for visibility and transmission loss of EM energy through battlefield obscurants have been important additions over the years to the target acquisition routines in virtual and constructive force on force combat simulations and aggregate war games. In the evolution of early US Army obscuration models probably the first successful effort was for the TRADOC CARMONETTE simulation in the early 1980's in support of Cost and Operational Effectiveness Analysis (COEA) studies of next generation

sensors and signature management technologies.

The Combined Obscuration Model for Battlefield Induced Obscurants (COMBIC) [ Hooock, Sutherland and Clayton, 1984] was introduced into CARMONETTE as a single integrated model for explosive crater and artillery dust, vehicular dust, military screening smoke pots, self-screening grenades, artillery-delivered smoke, diesel fire smoke, generator disseminated fog oil smokes and specialized screeners and moving sources. The model pre-computed off line all the physics-based processes and optical properties for

## Report Documentation Page

*Form Approved  
OMB No. 0704-0188*

Public reporting burden for the collection of information is estimated to average 1 hour per response, including the time for reviewing instructions, searching existing data sources, gathering and maintaining the data needed, and completing and reviewing the collection of information. Send comments regarding this burden estimate or any other aspect of this collection of information, including suggestions for reducing this burden, to Washington Headquarters Services, Directorate for Information Operations and Reports, 1215 Jefferson Davis Highway, Suite 1204, Arlington VA 22202-4302. Respondents should be aware that notwithstanding any other provision of law, no person shall be subject to a penalty for failing to comply with a collection of information if it does not display a currently valid OMB control number.

1. REPORT DATE <b>2007</b>	2. REPORT TYPE	3. DATES COVERED <b>00-00-2007 to 00-00-2007</b>	
4. TITLE AND SUBTITLE <b>Modeling Obscurants in an Urban Environment</b>		5a. CONTRACT NUMBER	
		5b. GRANT NUMBER	
		5c. PROGRAM ELEMENT NUMBER	
6. AUTHOR(S)		5d. PROJECT NUMBER	
		5e. TASK NUMBER	
		5f. WORK UNIT NUMBER	
7. PERFORMING ORGANIZATION NAME(S) AND ADDRESS(ES) <b>U.S. Army Research Laboratory, Computational and Information Sciences Directorate, AMSRD-ARL-CI-ED, White Sands Missile Range, NM, 88002</b>		8. PERFORMING ORGANIZATION REPORT NUMBER	
9. SPONSORING/MONITORING AGENCY NAME(S) AND ADDRESS(ES)		10. SPONSOR/MONITOR'S ACRONYM(S)	
		11. SPONSOR/MONITOR'S REPORT NUMBER(S)	
12. DISTRIBUTION/AVAILABILITY STATEMENT <b>Approved for public release; distribution unlimited</b>			
13. SUPPLEMENTARY NOTES <b>ITEA 2007 Modeling &amp; Simulation Conference, Las Cruces, NM, Dec. 10-13, 2007</b>			
14. ABSTRACT <b>Line of Sight obscuration effects of smoke, dust and debris on target acquisition are difficult to model in an urban environment. Wind flow and buoyancy in urban street canyons can be complex. This paper outlines the obscuration model being developed by the U. S. Army Research Laboratory for the NATICK RDEC to support the next generation of the Infantry Warrior Simulation (IWARS). It uses the legacy COMBIC obscuration model sources and STABIC concentration redistribution approach to simulating turbulence effects. The ARL-developed mass-consistent urban 3D Wind Field (3DWF) model is used to provide urban wind field inputs. Various techniques are described to adjust aerosol cloud concentrations for the effects of buildings as they confine the cloud to the streets.</b>			
15. SUBJECT TERMS			
16. SECURITY CLASSIFICATION OF:			17. LIMITATION OF ABSTRACT
a. REPORT <b>unclassified</b>	b. ABSTRACT <b>unclassified</b>	c. THIS PAGE <b>unclassified</b>	<b>Same as Report (SAR)</b>
			18. NUMBER OF PAGES <b>15</b>
			19a. NAME OF RESPONSIBLE PERSON

selected source types into pre-exercise “tabulated history files”. These were accessed during actual simulation as table lookup, so that calculations during each simulation replication could concentrate on computing the resulting overall transmission losses between potential targets and observers over four wavelength bands and two laser wavelengths. Each replication often integrated over tens of thousands of LOS relative to the geometry and locations of dozens of obscurant clouds active at any given time. These results reduced the maximum target acquisition range or the probability of target detection, identification and recognition that determined the “roll of the dice” outcomes deciding combat weapons engagements.

The present author was one of the primary developers of COMBIC and designed the model based on US Army TRADOC general specifications. This guidance included two major simplifications that were totally appropriate at the time for Cold War scenarios on open rolling terrain. First was a restriction that a single prevailing wind direction would be used and thus all clouds transport in one direction only, with the clouds being terrain-following in the vertical. And the obscuration effects must be totally deterministic and repeatable from replication to replication. This resulted in use of 10-minute time averaged Gaussian cloud distributions with no stochastic fluctuation or turbulence simulations.

Later combat simulations such as CASTFOREM implemented COMBIC, or in the case of JANUS and OneSaf used even more simplified models that were derived from COMBIC. But, with

Army Transformation came a change in doctrine. Engagements would no longer avoid urban and built-up areas. Non-linear combat would exploit technology advantages in night time operations and ISR even in complex forest, jungle and mountainous terrain. The restrictions of COMBIC to straight line transport and smooth Gaussian behavior obviously could not cope with variable urban wind fields; and a stochastic turbulent structure model (for simulating holes and thick spots in clouds) was developed but never funded for implementation.

The present paper outlines a new attempt to develop a comparable Urban Dust and Smoke Obscuration Model (UDSOM) focused on support for dismounted infantry operations, but also capable of supporting larger area effects.

## **2. IMPACTS OF OBSCURANTS IN URBAN AND COMPLEX TERRAIN**

Direct Line of Sight (LOS) target acquisition ranges in urban and complex terrain are dominated by the obviously shorter building-free, vegetation-free and terrain-limited LOS distances in these environments. These are often well within the longer range limits imposed by an image sensor resolution or the maximum range in open and gently rolling terrain range for detecting a EO/MMW or acoustic signal transmitted directly over an LOS.

Obscurants such as smoke and dust whether natural, intentional or the result of explosions, helicopter downwash and vehicle traffic further reduce target-background contrast and propagated EO energy. As airborne dust, aerosols

and other harmful agents spread over large areas they can impact ground operations not only by reducing visibility but also by potentially contributing to respiratory stress, environmental contamination and public concern. Downwind transport and dispersion of aerosol concentrations are treated by several existing environmental models used for hazard warnings and assessments. We do not intend to develop new sub modules to replace or compete with these existing models.

But obscuring clouds are also very important in urban and complex terrain for their local role as airborne screens. These can provide temporary cover, conceal movement, support deception, protect from lasers, act as counter measures to smart munitions, and be useful as signals or intelligence cues.

In these roles one important feature of obscuring screens is maintaining a size, duration and integrity of the screening effect at relevant sensor wavelengths. That is, the screen must reduce transmission to virtually zero throughout the screen at appropriate wavelengths for a predictable time interval. The challenge is to model not only the influence of local environment but also to model the statistical variations that can give rise to holes or features that compromise the screen.

A second important feature of interest is the visible size of a local airborne cloud itself. For example, a column of vehicles may be detected through their dust or diesel smoke plumes long before they become visible themselves. The feature of interest in this case is how long the local cloud transmission will remain below some maximum

transmission threshold above which the cloud can not be detected against its background.

The various features of the UDSOM urban obscuration model are:

- (1) Input of a grid of 3D, time-dependent urban wind field data for the aerosol transport.
- (2) Representation of all clouds as a sequence of puffs that expand downwind based on existing sub-models for urban cloud dispersion.
- (3) Efficient, fast Line of Sight transmission algorithms for multiple puff contributions.
- (4) Appropriate corrections to cloud concentration for cloud confinement by buildings and vegetation.
- (5) Use of a "streamline simulation" approach and its Time of Flight representation of flow for puff trajectories.
- (6) Reuse and extension of the COMBIC obscurant source models for smoke and dust, including wavelength-dependent optical properties
- (7) Modeled cloud buoyant rise and internal temperature and humidity, hygroscopic particle growth, evaporation, settling and deposition removal processes.
- (8) Simulation of the effects of turbulence on local variations in cloud concentration and structure.

Each of these features is discussed in more or less detail in the next sections.

### **3. URBAN WIND FIELD INPUT DATA**

The baseline obscurant clouds will be represented in UDSOM by a sequence

of Gaussian puffs that are advected by the wind. Wind fields in urban domains can be complex and changing. Therefore the model will rely on the input of a time-dependent, 3 dimensional wind field data set.

This grid of data could come from any source, potentially ranging from Computational Fluid Dynamics model output to Doppler Lidar measurements.

However, for current purposes the model will use output from a fast 3D Wind Field (3DWF) model developed by Dr. Yansen Wang of the US Army Research Laboratory, Adelphi, MD [Wang, Mercurio, Williamson and Garvey, 2003].

The current 3DWF model is a high resolution diagnostic model based on a variational analysis using mass conservation as a constraint. Its main attraction is the ability to produce results comparable to other urban wind models but at much shorter cpu times. A fast (one to two minutes for a 2 million grid

point volume) multi grid numerical method is employed to simulate microscale wind flow in complex terrain (such as within forest canopies) and all the way down to street level within urban terrain [Wang, et. al., 2005]. The 3DWF model inputs include high resolution terrain elevations, detailed building geometry data, vegetation height and leaf area index, and vertical wind profiles at one or more points.

The ability of the model to replicate wind tunnel features for flow over individual structures is shown in Figure 1. Examples of 3DWF wind fields for the Joint Urban 3000 experiment at Oklahoma City are shown in Figures 2 and 3 as an overhead view. Buildings are the dark areas. The model introduces time sequences of individual solutions based on input forecast or measured mean prevailing winds at one or more points. A new version of the model is being developed to include additional physics including eventual prognostic time-dependent modeling.

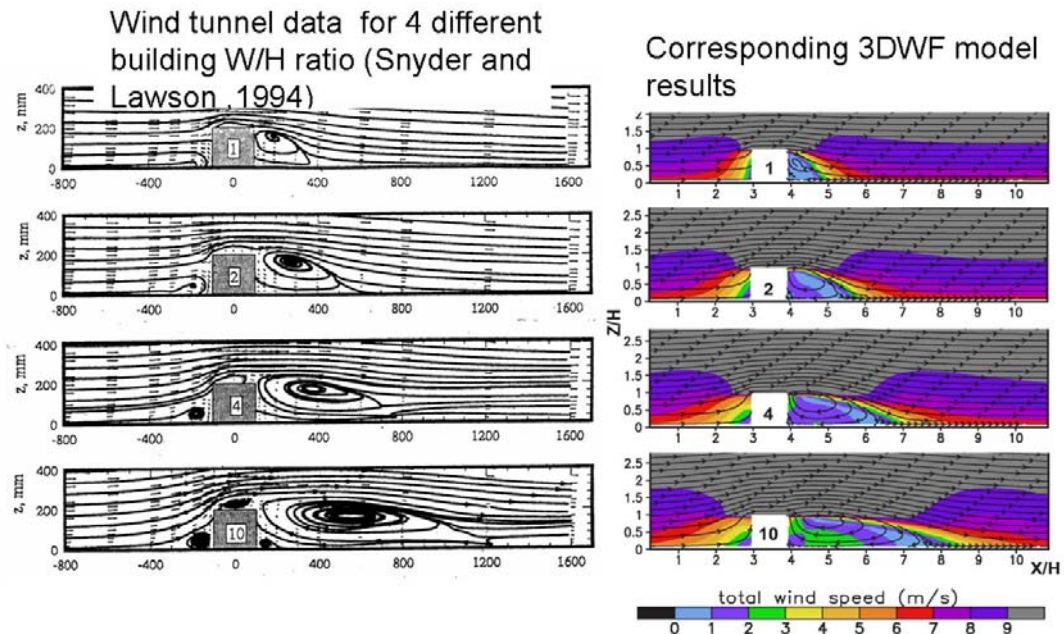


Figure 1. Comparisons of 3DWF output to wind tunnel results for flow over buildings (Y. Wang)

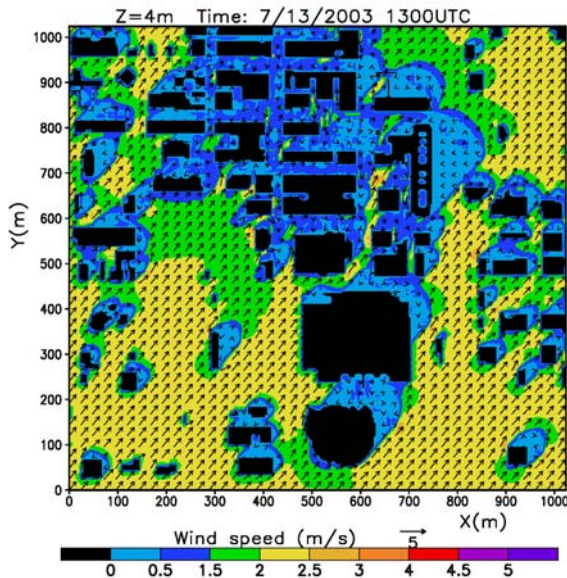


Figure 2. 3DWF wind fields modeled for Oklahoma City in JU2003 field experiments (Y. Wang)

#### 4. CLOUD DISPERSION MODEL

As the cloud puffs move downwind they will expand through the influence of turbulent mixing with ambient air and diffusion. At this time an existing urban dispersion model has not been chosen for use in UDSOM. It is possible that dispersion factors will be treated as input data fields to the UDSOM urban obscuration model so that different dispersion effects can be included.

For example, The current 3DWF model is to be extended this year to couple it to a Lagrangian Stochastic Particle Model (LSPM). This can be one candidate for the UDSOM.

#### 5. FAST LINE OF SIGHT INTEGRATION

Transmittance is an input to target acquisition algorithms to compute the effects of the atmosphere on target and background thermal signatures and contrast. Transmittance over the LOS from the target to the observer is the

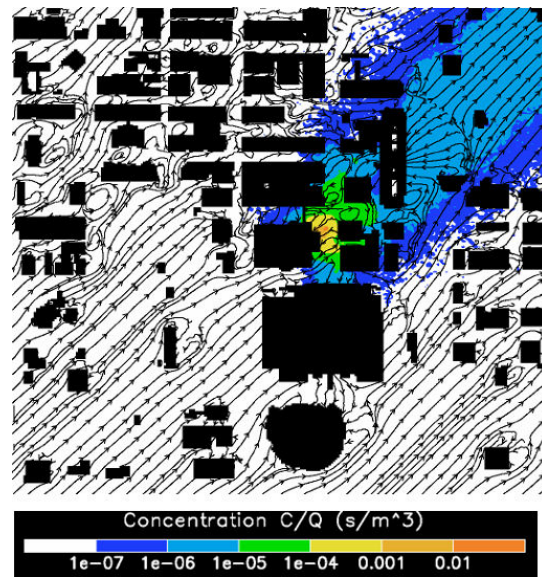


Figure 3. 3DWF wind stream lines modeled for Oklahoma City in JU2003 (Y. Wang).

primary output of the UDSOM model. It quantifies the effects of the atmosphere on attenuating target and background thermal signatures and visual or infrared thermal contrast. Transmittance  $T$  (with a range of values from zero to one) quantifies the transparency of the cloud for the relevant wavelength(s) of the sensor and can be computed from:

$$T = e^{-\alpha \cdot CL} \quad (1)$$

Mass extinction  $\alpha$  ( $\text{m}^2 \text{g}^{-1}$ ) is a bulk obscurant optical property (the optical loss per m per unit airborne aerosol mass concentration in  $\text{g m}^{-3}$ ). It varies with obscurant material (white phosphorus, fog oil, diesel smoke, missile exhaust plume, vehicular dust, explosive dust, etc.), sensor wavelength(s), and airborne particle size distribution(s). Many of these factors can be found in the IR and EO Systems Handbook [Hoock and Sutherland, 1991].

The total amount of obscurant over the LOS is called the Concentration-length product (CL in  $\text{g m}^{-2}$ ) and is more

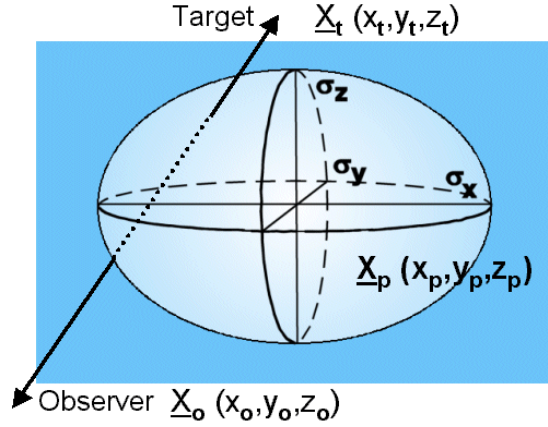


Figure 4. The Gaussian ellipsoidal puff accurately the path integral of concentration  $C$  over the LOS:

$$CL = \int_{\vec{x}_t}^{\vec{x}_o} C(\vec{x}) dl \quad (2)$$

A fast algorithm to compute CL between a target at  $X_t$  and observer located at  $X_o$  through a Gaussian puff has been developed. It is computed as follows.

For an ellipsoidal Gaussian puff, as depicted in Fig. 4, the concentration  $C$  ( $\text{g m}^{-3}$ ) at any point in space  $(x, y, z)$  is defined as:

$$C(x, y, z) = \frac{M_{puff}}{(2\pi)^{3/2} \sigma_x \sigma_y \sigma_z} \times \exp\left\{-\frac{1}{2} \left[ \left( \frac{x-x_p}{\sigma_x} \right)^2 + \left( \frac{y-y_p}{\sigma_y} \right)^2 + \left( \frac{z-z_p}{\sigma_z} \right)^2 \right] \right\} \quad (3)$$

Point  $X_p(x_p, y_p, z_p)$  is the position of the puff center and  $\sigma_x, \sigma_y, \sigma_z$  are the semi-axis standard deviations that define the size of the cloud.  $M_{puff}$  (g) is the total mass of obscurant in the puff and the

result of integrating  $C(x,y,z) dx dy dz$  over the entire volume of the cloud.

As shown in detail in earlier papers [Hoock, 2000a; and Hoock, Luces and Cionco, 2000b], every point  $(x, y, z)$  on the LOS satisfies parametric equations in terms of observer position  $(x_o, y_o, z_o)$ , target position  $(x_t, y_t, z_t)$  and distance  $s$  along the LOS from the observer to the target as:

$$x = x_o + \alpha s, \quad y = y_o + \beta s, \quad z = z_o + \gamma s \quad (4)$$

for  $0 \leq s \leq R$ , where  $R$  is the range (m) between observer and target. The range  $R$  and direction cosines  $(\alpha, \beta, \gamma)$  are constants for the specified LOS:

$$\alpha = \frac{x_t - x_o}{R}, \quad \beta = \frac{y_t - y_o}{R}, \quad \gamma = \frac{z_t - z_o}{R} \quad (5)$$

$$R = \sqrt{(x_t - x_o)^2 + (y_t - y_o)^2 + (z_t - z_o)^2} \quad (6)$$

Using these definitions, one can mathematically transform the ellipsoidal puff into a spherical puff while maintaining a straight line of sight:

$$\vec{\Omega}' = \left( \frac{\alpha}{\sigma_x} \right) \hat{i} + \left( \frac{\beta}{\sigma_y} \right) \hat{j} + \left( \frac{\gamma}{\sigma_z} \right) \hat{k} \quad (7)$$

$$\vec{X}'_{LOS} = \vec{X}'_o + s \vec{\Omega}', \quad \vec{X}'_{op} = (\vec{X}'_p - \vec{X}'_o) \quad (8)$$

$$D' = \left| \vec{\Omega}' \times \vec{X}'_{op} \right| / \left| \vec{\Omega}' \right| \quad (9)$$

One can then analytically solve for the line of sight CL through a puff as an exact solution based on eight values:

$$CL = \frac{M_{puff} \cdot [\Phi(R'_t) - \Phi(R'_o)]}{(2\pi)\sigma_x\sigma_y\sigma_z|\vec{\Omega}'|} \exp\left(-\frac{1}{2} \cdot D'^2\right) \quad (10)$$

where the distances along the LOS from the closest point to the center of the cloud to the observer  $R'_o$  and to the target  $R'_t$  respectively are

$$R'_o = -\vec{\Omega}' \cdot \vec{X}'_{op} / |\vec{\Omega}'| \quad (11)$$

and

$$R'_t = R'_o + R |\vec{\Omega}'| \quad (12)$$

When the target and observer are on opposite sides of the entire cloud then the term in brackets in the numerator is one and can be ignored. (This occurs for example if  $R'_o$  is a large negative value and  $R'_t$  is a large positive value.) But, if the target is inside the cloud or the observer is inside the cloud, or both, then this term provides the correction factor through the function  $\Phi(R')$ , as shown in Figure 5. It is the Cumulative

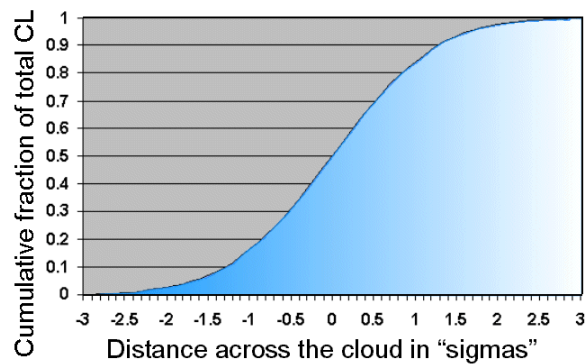


Figure 5. Cumulative Normal function  $\Phi(R')$

Normal distribution and varies from 0 to 1 as the observer and target points are moved across the cloud.  $\Phi$  is an intrinsic computer routine found with most compilers or as part of the random number or statistical routine libraries.

This transformed solution for CL is particularly efficient to compute, and it is also important because it simplifies the corrections needed to account for the interactions of the ellipsoidal Gaussian puffs with urban walls, ground plane and building tops.

#### 4. BUILDING, VEGETATION AND ROADWAY EFFECTS ON CLOUD CONCENTRATIONS

The mathematical transformations of the last section are also very useful when accounting for the explicit effects of building and roadway surfaces that confine the cloud to the street “canyons”. A correction factor can be computed to estimate the amount of cloud mass that would have mathematically ended up sharing a 3D region occupied by a building or “below” the street surface as shown as the cross-hatched area in Figure 6. This mass can be redistributed into the puff to conserve the mass of airborne

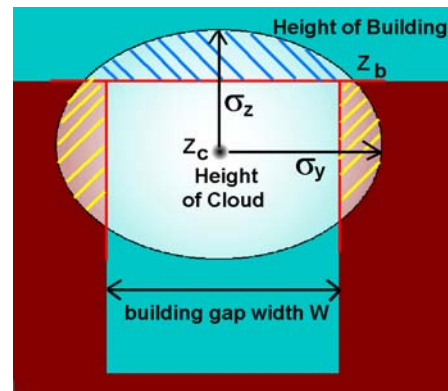


Figure 6. Accounting for cloud confinement factors

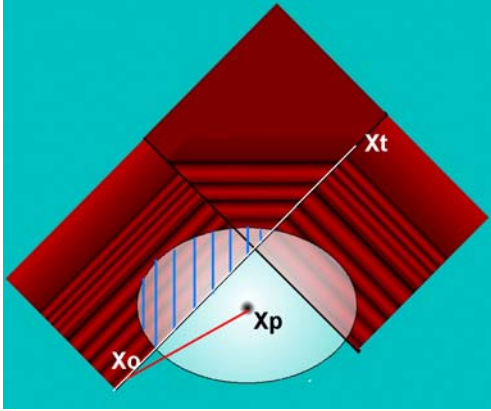


Figure 7. Cloud interaction with a wall.

obscurant participating in LOS transmission loss.

As an example, Figure 6 is a side view of a cloud confined in a street canyon of width  $W$  by two building vertical walls (brown areas) of height  $Z_b$ . The exact mass of obscurant that needs to be distributed back into the urban canyon is easily shown to be:

$$M_{refl} = M_{puff} \cdot \Phi\left(\frac{(Z_b - Z_c)}{\sigma_z}\right) \cdot 2 \cdot \left[1 - \Phi\left(\frac{W}{2 \cdot \sigma_y}\right)\right] \quad (13)$$

A more challenging situation is shown in Figure 7 where the cloud is rotated with respect to the building surface. This figure shows a top down view of a cloud interacting with two walls of a building (brown regions). Given the puff center at  $X_p$ , and two points  $X_t$  and  $X_o$  at the same height above ground as the cloud that define the wall boundary, we can apply the transformation equations of the last section. The mass of obscurant beyond one of the wall boundaries (shown as a cross hatched area) that must be “reflected” back into the cloud in the street can be computed exactly as:

$$M_{refl} = M_{puff} \cdot [1 - \Phi(D')] = M_{puff} \cdot \left[1 - \Phi\left(\frac{|\vec{\Omega}' \times \mathbf{X}_{op}|}{|\vec{\Omega}'|}\right)\right] \quad (14)$$

$D'$  is actually the perpendicular distance (in sigma units) from the puff center to the wall in the transformed frame, and  $\Phi(D')$  is the cumulative normal distribution value.

These types of corrections are only possible if the exact positions, orientations and dimensions of the building structures are known. More generally one may not have time to work out this level of detail. It may be enough to know only the “areal density” of buildings or vegetation within a grid of say 100m x 100m or perhaps 50m x 50m cells. This approach is called the use of Morphology Statistics for built up areas. Figure 8 is a table of the density distributions for different classes of buildings at Salt Lake City and was presented in detail in the 2002

Building Fractional Area Density by UTZ														
Building Densities (%) by Each UTZ Category for Salt Lake City (Cat 1-3 and 18 omitted)														
% Den	Cat 4	Cat 5	Cat 6	Cat 7	Cat 8	Cat 9	Cat 10	Cat 11	Cat 12	Cat 13	Cat 14	Cat 15	Cat 16	Cat 17
0	0	0	0	0	0	0	1	6	0	0	0	0	10	22347
10	6	1	24	42	1491	11	21	9	31	328	384	75	144	6
20	0	0	100	102	3374	16	82	62	73	900	608	84	310	15
30	7	4	101	180	3281	9	67	73	78	849	615	75	278	6
40	0	6	59	75	692	6	31	35	51	159	335	42	158	3
50	0	0	72	44	60	10	22	38	29	46	251	18	123	1
60	1	5	43	12	16	4	17	24	16	9	226	20	98	1
70	1	0	29	11	4	2	12	19	9	1	183	27	86	0
80	0	0	46	18	2	6	15	11	3	0	182	14	96	1
90	1	1	6	1	3	4	4	7	0	0	69	9	29	0
100	1	0	84	2	1	2	1	31	3	0	123	17	53	0

Urban Terrain Zones (UTZ)	
Code	Description
1 - 5	Attached: Central Business District, high rise apartments, row houses, industry and commercial string streets
6 - 10	Detached, Closely Spaced: office complexes, apartments, houses, industry, commercial
11 - 16	Detached, Widely Spaced: shopping centers, planned apartments, houses (expensive and inexpensive), industry/storage/office complexes, commercial, administrative/cultural/school
17	Non-buildings

Figure 8 Salt Lake City areal density distributions

ITEA paper [Hoock and Cionco, 2002c].

Here we simply recap that if the density of buildings and vegetation in terms of their area and heights are known then the volumes of cloud excluded by these features can be estimated. Figure 9 shows this approach in terms of the equivalent size of an ellipsoidal cloud of radii  $2.15\sigma$  relative to the morphology cell size and areal density of buildings and vegetation. Details were discussed in detail in the related ITEA paper of 2002 [Hoock and Cionco, 2002c].

## 5. STREAMLINE SIMULATION

Interestingly, geologists and crude oil production developers have addressed an analogous problem during years of modeling the flow of oil under pressures set up by injection wells that push oil toward collectors or production wells. Considerable funding has been expended by industry and in academic research, and an informative review of the use of Streamline Based Flow Simulation in solving flow in large, geologically heterogeneous and complex systems, is available on-line from [Thiele, 2001].

Our interest in this approach is that it parallels the old COMBIC philosophy of pre-computing a cloud trajectory “history” file. If we tabulate the time that it takes for the cloud centroid to move

Uniform Ellipsoidal Puff Cloud Concentration

$$C_{Avg} = \frac{3M_{puff}}{4\pi(2.15)^3\sigma_x\sigma_y\sigma_z}$$

Cloud Puff Center at  $(X_C, Y_C, Z_C)$   
And Cloud Size Std. Dev. Of  $\sigma_x, \sigma_y, \sigma_z$

- Case 1: Cloud size is much larger than the grid cell

$$M_{refl} = C_{Avg} \cdot A_{cell} \cdot f_{build} \cdot [z_b - (z_c - 1.733 \cdot \sigma_z)]$$

where  $A_{cell}$  = Area of the cell

$z_b$  = Height of the building

and  $f_{build}$  = Building fractional areal density

- Case 2: Cloud size is comparable to street canyons in the grid cell

$$M_{refl} = C_{Avg} \cdot (3.466)^2 \sigma_x \sigma_y \cdot f_{build} \cdot [z_b - (z_c - 1.733 \cdot \sigma_z)]$$

- Case 3: Cloud size is much smaller than the grid cell:

Perform LOS calculation with no correction needed for building interaction

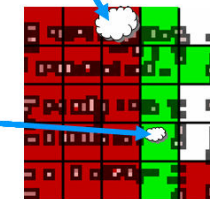
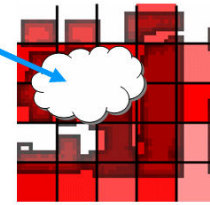


Figure 9. Correction factors for building morphology effects on concentrations

downwind different distances along a velocity streamline such as those shown in Figure 3, then it is a simple matter to subtract that time from the current wall clock time to determine how much obscurant was produced at that earlier moment based on the munition time-dependent burn or “emission profile”.

The similar methodology in Streamline-Based Flow Simulations is to compute the 3D trajectory and the Time of Flight and other properties (in our case cloud size, for example) as 1D tabulations along the streamline. The streamline itself can be determined from Pollock’s 3D tracing method through a Cartesian cell [taken from Thiele, 2001]. Given an arbitrary entry point, the time to exit and the exit point can be determined analytically (from Batycky et al. 1997) as follows. Assume the velocity  $V_{x0}$  is the velocity entering a grid cell as determined from the flow rate or simply as the wind velocity along the streamline at that point. Then

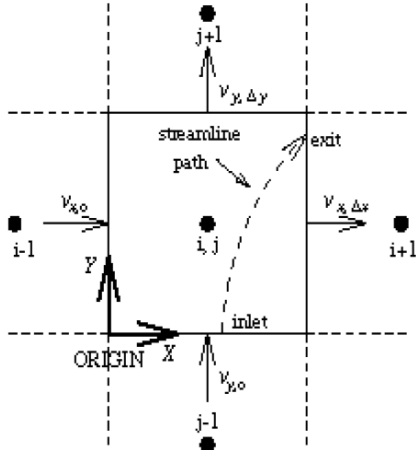


Figure 10. Batycky Streamline Algorithm

$$v_x = v_{x0} + g_x(x - x_0); \quad g_x = \frac{v_{x\Delta x} - v_{x0}}{\Delta x} \quad (15)$$

and similarly for y and z where  $g_x$  is the velocity gradient in the x-direction.

The exit time from the cell will be the smallest of the values

$$\Delta t_z = \frac{1}{g_z} \ln \left[ \frac{v_{z0} + g_z(z_e - z_0)}{v_{z0} + g_z(z_i - z_0)} \right]$$

$$\Delta t_y = \frac{1}{g_y} \ln \left[ \frac{v_{y0} + g_y(y_e - y_0)}{v_{y0} + g_y(y_i - y_0)} \right]; \quad (16)$$

$$\Delta t_x = \frac{1}{g_x} \ln \left[ \frac{v_{x0} + g_x(x_e - x_0)}{v_{x0} + g_x(x_i - x_0)} \right];$$

And thus the position of the exit point will be based on the  $\Delta t_m = \min\{\Delta t_x, \Delta t_y, \Delta t_z\}$  with the smallest time:

$$x_e = \frac{1}{g_x} \ln[v_{xi} \exp(g_x \Delta t_m) - v_{x0}] + x_0$$

$$y_e = \frac{1}{g_y} \ln[v_{yi} \exp(g_y \Delta t_m) - v_{y0}] + y_0$$

$$z_e = \frac{1}{g_z} \ln[v_{zi} \exp(g_z \Delta t_m) - v_{z0}] + z_0 \quad (17)$$

The geologists then proceed to show that the 1D solutions of oil flow along the flow lines is simpler and faster for many simulations than solving 3D finite difference equations. We intend to use streamlines as the basis for book keeping of the trajectories of cloud puffs. And one can note that there are other parallels such as assuming the buildings are obstructions and the space between them are “pores” so that an equivalent “interstitial flow” can be identified with the smoke concentrations corrected for building density effects.

## 6. SOURCE CHARACTERISTICS

COMBIC will be a rich source of obscurant characteristics as shown in Figures 11 and 12. There are also several other tables that identify other characteristics such as the initial cloud radius, the obscurant mass emission rate profiles and burn durations, the thermal production rates of munitions, etc. However, other additional sources are also expected to be part of the urban debris that may need to be modeled, and the increased use of colored smokes may affect transmission over the visual band and require additional characterization.

## 7. CLOUD BUOYANCY AND CLOUD PHYSICS

There are a number of dynamic processes that affect cloud characteristics and trajectories. One of the major ones is cloud thermal buoyancy.

If clouds remained at ambient air temperature then they would follow the ambient wind velocity streamlines quite well. However, the thermal energy released in explosions and in the chemical reactions of smoke as they burn to produce an aerosol definitely can affect cloud rise. In addition some smoke generators expel smoke from a turbine air outlet that provides an initial momentum jet that similarly can project the cloud upward initially.

We choose to continue to use the buoyancy and entrainment model in COMBIC as a versatile method to compute the rise, cooling and expansion of fireballs and warm clouds resulting from exothermic reactions that generate aerosol particles in the air. The four quantities computed are the time change in cloud temperature to ambient temperature, the fractional increase in cloud total air mass, the upward acceleration and the horizontal acceleration respectively.

$$\frac{d}{dt} \left( \frac{T}{T_a} \right), \frac{1}{m} \frac{dm}{dt}, \frac{dw}{dt}, \text{ and } \frac{du}{dt} \quad (18)$$

These four quantities can be determined using four equations: conservation of horizontal and vertical momentum, cloud internal energy and the entrainment of

Obscurant		Wavelength ( $\mu\text{m}$ )						
Type	Name	.4-.7	.7-1.2	1.06	3 to 5	8 to 12	10.6	94 GHz
1.	White phosphorus	(See figure B.3)						
2.	PWP, WP wedges	(See figure B.3)						
3.	Hexachloroethane	(See figure B.4)						
4.	Fog oil	6.851	4.592	3.479	0.245	0.020	.018	0.001
5.	Red phosphorus	(See figure B.3)						
6.	IR (generator)	1.860	1.630	1.400	1.790	1.680	.680	0.001
7.	IR (munition)	1.860	1.630	1.400	1.790	1.680	.680	0.001
8.	Diesel fuel	5.650	4.080	3.250	0.245	0.023	0.027	0.001
9.	Vehicular dust	0.320	0.300	0.290	0.270	0.250	0.250	0.001
10.	HE dust, small	0.320	0.290	0.260	0.270	0.260	0.240	0.001
11.	HE dust, large	0.035	0.036	0.037	0.035	0.038	0.036	0.002
12.	Carbon debris	1.500	1.460	1.420	0.750	0.320	0.300	0.001
13.	HE dust, ballistic	0.001	0.001	0.001	0.001	0.001	0.001	0.0004
14.	Diesel/oil/rubber	6.100	3.750	2.94	1.350	1.010	1.000	0.002
15.	Fog oil/kerosene	6.851	4.592	1.430	0.054	0.020	0.018	0.001
16.	PEG 200	5.370	2.900	2.100	0.090	0.090	0.070	0.001
17.	Anthracene	6.200	3.500	2.500	0.230	0.050	0.048	0.001
18.	FS	3.330	2.750	2.660	0.260	0.320	0.230	0.001
19.	FM	1.300	1.740	1.700	0.080	0.160	0.380	0.001
20.	IR (M76)	1.000	1.000	1.000	1.000	1.000	1.000	0.001
21.	O.A. Brass	1.300	1.400	1.400	1.400	1.400	1.400	0.001
22.	GRAPH7525	1.800	2.000	2.000	2.000	2.000	2.000	0.001
23.	Kaolin	2.000	1.000	1.000	0.100	0.400	0.400	0.001
24.-30.	User-defined	User-defined						

Figure 11. The mass extinction values for COMBIC obscurants

Munition Type	Fill Weight	Source Code	Efficiency	Obsc. Code	# of Sub-munitions
155-mm HC M1 canister	5.40	1	70	3	1
155-mm HC M2 canister	2.80	2	70	3	1
105-mm HC canister	1.57	3	70	3	1
155-mm HC M116B1 projectile*	19.00	4	70	3	4
105-mm HC M84A1 projectile*	4.73	5	70	3	3
Smoke pot, HC M5*	31.00	6	70	3	1
Smoke pot, HC M4A2*	27.00	7	70	3	1
60-mm WP M302A1 cartridge*	0.76	8	100	1	1
81-mm WP M375A2 cartridge*	1.60	9	100	1	1
4.2-in WP M328A1 cartridge*	8.14	10	100	1	1
2.75-in WP M156 rocket*	2.12	11	100	1	1
155-mm WP M110E2 projectile*	15.60	12	100	1	1
105-mm WP M60A2 cartridge*	3.83	13	100	1	1
4.2-in PWP M328A1	8.14	14	60	2	1
5-in PWP Zuni MK4	13.52	15	60	2	1
2.75-in WP wedge	0.463	16	66	2	1
2.75-in WP M259 rocket*	4.63	17	66	2	10
3-in WP wick	0.139	18	71	2	1
6-in WP wick	0.234	19	67	2	1
155-mm WP M825 projectile*	16.43	20	74	2	116
81-mm RP wedge	0.128	21	53	5	1
I81-mm RP XM819 cartridge*	2.834	22	48	5	28
Generator, ABC M3A3*	10.0**	23	100	4	1
Generator, VEES*	11.0**	24	100	8	1
Smoke Pot, Fog Oil M7A1*	1.7**	25	100	4	1
155-mm HE (dust)***	14.9	26	-	10	1
105-mm HE (dust)***	6.04	27	-	10	1
4.2-in HE (dust)***	7.45	28	-	10	1
10-lb C4 (dust)***	13.4	29	-	10	1
Diesel fuel/oil/rubber fire	150.**	30	26	14	1
Muzzle Blast	2.00	31	-	10	1
M76 IR Grenade	2.98	32	60	20	1
L8A1/L8A3 Grenade	0.794	33	95	5	1

Figure 12 COMBIC characteristics of various obscurant sources

external air that is dependent on the cross sectional area and velocity of the puff.

The mass of the buoyant puff is

$$m_t = \frac{4}{3}\pi R_h^2 R_z \rho \quad (19)$$

assumed to be an ellipsoid of horizontal radius  $R_h$  and vertical radius  $R_z$  and the density of the air and debris mass is  $\rho$  resulting in total mass  $m_t$ .

Outside air entrains and mixes at a fractional mass rate of

$$\frac{1}{m} \frac{dm}{dt} = \mu \frac{\rho_a}{\rho} \frac{|\vec{v} - \vec{v}_a|}{R} \quad (20)$$

This is proportional to the difference in velocity between the puff and the ambient airflow per unit mean radius of the puff and  $\mu$  is an empirically derived parameter well established at a nominal value of 0.75 for puff entrainment.

Conservation of energy is based on thermal mixing and leads to the equation:

$$\frac{d}{dt} \frac{T}{T_a} = \left(1 - \frac{T}{T_a}\right) \frac{1}{m} \frac{dm}{dt} - \frac{s}{g} \left(\frac{T}{T_a}\right) w \quad (21)$$

Where  $g$  is the acceleration due to gravity and  $s$  is the static stability

parameter that defines the vertical change in potential temperature:

$$\begin{aligned} s &= \frac{g}{T_a} \frac{d\theta}{dz} \\ &= \frac{g}{T_a} \frac{dT_a}{dz} + \left(\frac{\gamma - 1}{\gamma}\right) \frac{g}{H_p} \end{aligned} \quad (22)$$

For stable (nighttime) atmospheres  $s$  is positive. For unstable (daytime) atmospheres  $s$  is negative; and for neutral conditions (cloud cover and high winds)  $s$  is zero.

Conservation of momentum is easily understood from the balance of forces in the equation:

$$\begin{aligned} \frac{d(mw)}{dt} &= m_a g - mg + w_a \frac{dm}{dt} \\ &\quad - \frac{1}{2} C_D \rho_a A_{\perp} (w - w_a) |w - w_a| \end{aligned} \quad (23)$$

Where the change in momentum (force) equals: the difference in the downward weight of ambient air minus the upward buoyant force of warm puff air; plus the “thrust” reaction term for the increased mass of entrained air; and finally the counter force of drag on the puff as it encounters air resistance to its cross sectional area  $A_{\text{perp}}$ . (The absolute value assures that the drag opposes motion of the puff.) The drag coefficient  $C_D$  is typically about 0.8.

The horizontal momentum equation is similarly:

$$\frac{d(mu)}{dt} = u_a \frac{dm}{dt} - \frac{1}{2} C_D \rho_a A_{\perp} (u - u_a) |u - u_a| \quad (24)$$

These momentum equations can be recast into the simpler forms:  
And

$$\frac{dw}{dt} = \left( \frac{T}{T_a} - 1 \right) g - \frac{1.4}{m} \frac{dm}{dt} (w - w_a) \quad (25)$$

$$\frac{du}{dt} = - \frac{1.4}{m} \frac{dm}{dt} (u - u_a) \quad (26)$$

These equations are solved simultaneously or using iterative improvements to settle down to a consistent set of values at each step in the buoyant puff rise.

Other physics based processes that are computed for the cloud are temperature profiles with time and growth of hygroscopic aerosol particles until they reach equilibrium between external water vapor pressure (humidity) and particle surface tension. The resulting increase in mass of the smoke produced is called the “yield factor”. This increase in smoke mass can include not only the water drawn from the air in particle growth, but often the increase in mass due to the “burn” or chemical oxidation process that generates the smoke. Particle growth at 100% humidity never goes to infinity because as the smoke withdraws moisture from inside the puff, the internal relative humidity will drop to some final value less than 100%. Entrainment of external humid air as the puff moves can introduce additional water vapor for growth.

## 8. SIMULATING CONCENTRATION FLUCTUATIONS

The final process that is modeled is the effect of natural atmospheric turbulence in generating cloud concentration fluctuations. A simulation model has been developed called the Statistical Texturing Application To Battlefield Induced Clouds (STATBIC). STATBIC comes in a 3D and a path integrated 2D version.

Basically STATBIC generates a fluctuation field that is not random but rather reproduces spatial correlations and structure functions that follow the Kolmogorov power spectrum (or in principle any chosen Hurst parameter).

Structure functions correlate the average squared concentration difference between one location and another separated by a fixed delta. Similarly, one can generate structure functions for the squared difference in a constant lag in time series:

$$\begin{aligned} \langle |C(t + \Delta t) - C(t)|^2 \rangle &= (\Delta t)^{2H} \sigma_t^2, \\ \langle |C(x + \Delta x) - C(x)|^2 \rangle &= (\Delta x)^{2H} \sigma_x^2, \end{aligned} \quad (27)$$

Where  $H = E - D$  is the Hurst parameter, the difference between the Euclidean dimension and the Fractal dimension of the process. For Kolmogorov statistics, which are known to apply to the eddy cascades over the inertial subrange of the atmosphere, the Hurst parameter  $H = 1/3$ . For uncorrelated Brownian motion  $H = 1/2$ .

When  $H$  is less than  $1/2$  a process is said to be positively correlated and this means that if a fluctuation is above the mean at one point then it is likely that the nearby fluctuations are also positive, that is, the fluctuations are relatively smooth. For Kolmogorov processes such as idealized atmospheric turbulence the opposite is true. The nearby fluctuations are likely to be anti-correlated and if there is a thick spot at one location there is likely to be a thin one nearby. This gives rise to holes in smoke clouds unless they are sufficiently extended in the line of sight direction to average over many such eddy fluctuations and thus “smooth out” the fluctuations. This is shown in Figure 13 where the STATBIC algorithm is applied to a smooth modeled Gaussian plume. It is less evident in the simulated puffs of Figure 14.



Figure 13: STATBIC textured Gaussian plume

Of course there is little reason to believe that urban turbulence is fully Kolmogorov. Measure programs are being undertaken to better understand the statistics in such environments, and STATBIC will be modified to accommodate different Hurst



Figure 14. STATBIC textured puff concentrations illuminated from above – note shadows

parameters and inner and outer scale effects.

## 9. CONCLUSIONS

This paper outlines an approach to develop a new Urban Dust and Smoke Obscuration Model (UDSOM) that brings together several sub module algorithms that have been developed over the last few years.

The model is expected to be coded and initially released over the next two years. Its focus will be on screening effects, dust and debris as they impact the operations of the urban soldier.

## 10. ACKNOWLEDGEMENT

The author wishes to acknowledge the contribution of Dr. Yansen Wang of the Army Research Laboratory whose 3DWF model outputs are used as examples for section 3 of this paper.

## 11. REFERENCES

Batycky, R.P., M.J. Blunt, M.J., and M. R. Thiele, 1997: “A 3D Field Scale Streamline-Based Reservoir Simulator,” SPE Reservoir Engineering (November 1997) 246-254.

- Hook, Donald, Robert Sutherland and Donna Clayton, 1984: "Combined Obscuration Model for Battlefield Induced Contaminants", U.S. Army Atmospheric Sciences Laboratory Technical Report TR-0160-11, USA ASL, White Sands Missile Range, NM.
- Hook, Donald W. and Robert A. Sutherland, 1993: "Obscuration Countermeasures", Volume 7, Countermeasure Systems, The Infrared & Electro-Optical Systems Handbook, David H. Pollock Editor, SPIE Optical Engineering Press, Chapter 6, pp 359-493.
- Hook, Donald W. Jr., 2002a: "New Transmission Algorithms for Modeling Obscurants in Urban Environments", in the Proceedings of the 70th MORSS - 18-22 June 2002, US Army Combined Arms Center, Ft. Leavenworth, KS; WG-11 (Military Environment Factors). Available on CD and partly accessible through the MORS web site. See abstracts at: [http://www.mors.org/publications/abstracts/70morss/11wg\\_abs.htm](http://www.mors.org/publications/abstracts/70morss/11wg_abs.htm) .
- Hook, Donald W. Jr., Saba (Lou) A. Lucas, and Ronald Cionco, 2002b: "Modeling Local Urban Meteorology for Smoke Obscuration", Proceedings of the Fall 2002 Simulation Interoperability Workshop, 9-13 Sept, 2002, Orlando, FL, Paper 02F-SIW-071.pdf available on CD or electronically online at: <http://www.sisostds.org/conference/index.cfm?conf=02FALL>.
- Hook, Donald and Ronald Cionco, 2003c: "Modeling Urban Smoke And Aerosol Effects Using Urban Morphology Statistics", in Proceedings of the 2002 ITEA Conference, Dec 2002, Las Cruces, NM.
- O'Brien, Sean and Donald Hook, 1998, "STABIC – A Method for Inclusion of Fractal Statistics in Obscurant Transport Models", US Army Research Laboratory Report ARL-TR-1375, April 1998, USARL, White Sands Missile range, NM 88002-5501.
- Thiel, Marco R., 2001, "Streamline Simulation", from Proceedings of the 6th International Forum on Reservoir Simulation, September 3rd-7th, 2001, Schloss Fuschl, Austria; but directly available from the web site link: <http://www.streamsim.com/index.cfm?go=streamlines.home>
- Thiel, Marco R., 2003, "Streamline Simulation", from Proceedings of the 7th International Forum on Reservoir Simulation, June 23-27, 2003, Baden-Baden, Germany; but directly available from the web site link: <http://www.streamsim.com/index.cfm?go=streamlines.home>
- Wang, Yansen, Jon Mercurio, Chatt Williamson, Dennis Garvey, 2003: "A High Resolution, Three Dimensional, Computationally Efficient, Diagnostic Wind Model: Initial Development Report", U.S. Army Research Laboratory Technical Report ARL-TR-3094, Oct 2003, ARL, Adelphi, MD.
- Wang, Yansen, Chatt Williamson, Dennis Garvey, Sam Chang and James Cogan, 2005: "Application of a Multigrid Method to a Mass-Consistent Diagnostic Wind Model" JAM, vol 44, no. 7, 2005, pp 1078-1089